

**Symmetries of the similarity renormalization group for nuclear forces**

V. S. Timóteo\*

*Faculdade de Tecnologia, Universidade Estadual de Campinas, UNICAMP, Limeira, SP 13484-332, Brazil*

S. Szpigel†

*Faculdade de Computação e Informática, Universidade Presbiteriana Mackenzie, São Paulo, SP 01302-907, Brazil*

E. Ruiz Arriola‡

*Departamento de Física Atómica, Molecular y Nuclear and Instituto Carlos I de Física Teórica y Computacional, Universidad de Granada, E-18071 Granada, Spain*

(Received 4 August 2011; revised manuscript received 2 July 2012; published 14 September 2012)

We analyze the role played by long-distance symmetries within the context of the similarity renormalization group (SRG) approach, which is based on phase-shift-preserving continuous unitary transformations that evolve Hamiltonians with a cutoff on energy differences. We find that there is a SRG cutoff for which almost perfect fulfillment of Wigner symmetry is found. We discuss the possible consequences of such a finding.

DOI: [10.1103/PhysRevC.86.034002](https://doi.org/10.1103/PhysRevC.86.034002)

PACS number(s): 21.30.-x, 05.10.Cc, 13.75.Cs

**I. INTRODUCTION**

The use of effective interactions in nuclear physics is rather old (for a review see, e.g., [1,2] and references therein). The basic idea is to emphasize the role of the physically relevant degrees of freedom, which in the case of nucleons in finite nuclei depends very much on the relevant energy scale or equivalently on the shortest de Broglie wavelength sampling the interactions. Moreover, the explicit effects of the (hard) core which traditionally induce strong short-distance correlations actually depend on detailed and accurate knowledge of the interaction at rather short distances (see, e.g., Ref. [3] and references therein).

While the issue of scale dependence is best formulated within a renormalization framework [4], Wilsonian methods have only been seriously considered as an insightful technique in the study of nuclear forces about a decade ago (for a balanced review see [5] and references therein).

Some years ago Glazek and Wilson [6,7] and independently Wegner [8] showed how high-momentum degrees of freedom can decouple while keeping scattering equivalence via the so-called similarity renormalization group (SRG). The SRG is a renormalization method based on a series of continuous unitary transformations that evolve Hamiltonians with a cutoff on energy differences. Such transformations are the group elements that give the method its name. By viewing the Hamiltonian as a matrix in a given basis, the similarity transformations suppress off-diagonal matrix elements as the cutoff is lowered, forcing the Hamiltonian toward a band-diagonal form. An important feature of the SRG is that all other operators are consistently evolved by the same unitary transformation. Quite generally the transformation may involve any number of particles and allows one to generate well-behaved multiparticle renormalized interactions. In Refs. [9,10],

the main features of the SRG formalism were illustrated by Perry and one of the present authors (SS) through simple examples from quantum mechanics, namely the Schrödinger equations for nonrelativistic two-body systems in one and two dimensions with Dirac-delta contact potentials.

Recently, the SRG has been applied to evolve several nucleon-nucleon ( $NN$ ) potentials to phase-shift-equivalent softer forms [11], which become extremely handy for many-body calculations in nuclear physics (for a review see, e.g., [12]). The role played by bound states on the SRG evolution has also been analyzed [13], and it was found that the SRG generator and evolution SRG scale may be suitably chosen to avoid undesirable singularities sneaking in and ruining the low-energy properties of the SRG-evolved interaction. This has been recently applied to prevent the spurious bound states which normally appear in meson exchange potentials [14]. The complicated neutron-nucleus scattering becomes far simpler within a SRG perspective [15]. A general discussion of operator evolution and in particular deuteron properties has also been carried out where a link to the operator product expansion has been envisaged [16].

A great advantage of the SRG method over other approaches such as the  $V_{\text{low}k}$  [1] or the unitary correlation operator method (UCOM) method [17] is the straightforward application to the scale dependence of few-body forces [18,19] which consistently treat two-body-induced as well as initially introduced few-body interactions (see Ref. [20] for a discussion on simple one-dimensional models). A further main advantage of SRG is the tremendous reduction of the many-body problem, since effectively the two-body interaction becomes almost diagonal and consequently the corresponding phase space gets enormously reduced. This of course is done at the cost of allowing three- or even four-body forces, which precisely due to the high-energy decoupling of the SRG remain shorter range than the two-body effective interaction but with a different, scale-dependent strength. The connection to the UCOM configuration space method was discussed in Refs. [21,22] where it was shown how a suitable rescaling of the radial coordinate is in fact equivalent to choosing a static generator.

\*varese@ft.unicamp.br

†szpigel@mackenzie.br

‡earriola@ugr.es

The relation of the SRG to the  $V_{\text{lowk}}$  method was discussed in Ref. [23] as a block diagonal cutoff representation with a Hilbert space with high- and low-momentum components where the mixing between off-diagonal elements becomes negligible along the SRG evolution.

The momentum-space  $V_{\text{lowk}}$  approach [24] (see, e.g., Ref. [12] for a review) takes a Wilsonian point of view of integrating out high-energy components. This allows one to obtain a self-adjoint  $V_{\text{lowk}}$  potential from a bare potential,  $V$ . Given a symmetry group with a generic generator  $X$ , standard symmetry means that  $[V, X] = 0$  implies  $[V_{\text{lowk}}, X] = 0$ . The reverse, however, is not true. We define a *long-distance symmetry* as a symmetry of the effective interaction, i.e.,  $[V_{\text{lowk}}, X] = 0$  but  $[V, X] \neq 0$ . From a renormalization viewpoint that corresponds to a symmetry of the potential broken only by short-distance counterterms. This is discussed at length in Refs. [25–27] and summarized in Ref. [28]. On the other hand, when the interaction is itself evolved to low energies the symmetry of the long-range part of the potential reappears explicitly for the  $V_{\text{lowk}}$  potential.

In a recent work it has been made clear that the momentum-space  $V_{\text{lowk}}$  approach [24] displays a remarkable symmetry pattern, which in the case of Wigner SU(4) spin-isospin symmetry with nucleons in the fundamental representation may be related unambiguously to large- $N_c$  dynamical features of QCD [29], as analyzed in detail in Refs. [25–28]. This possibility of linking a very distinct pattern of QCD to an observable feature of the  $NN$  interaction is extremely intriguing. However, the symmetries are very well satisfied and a constructive point of view is to select what definitions of the effective interaction comply with the symmetries. Of course, we do not expect them to be perfect, but given the fact that in the  $V_{\text{lowk}}$  (the diagonal elements) approach they work so well, it is worth testing other definitions. We want to analyze whether the currently used SRG complies with the symmetry pattern. In a previous work by one of the present authors (ERA) [30] the running scale dependence of the effective interaction was carried out at low momenta with the sole input of low-energy scattering parameters such as scattering lengths (volumes) and effective ranges. It was found that the mixing induced by the tensor force was essential to achieve the Wigner symmetry condition. It was also found that Wigner symmetry sets in at a scale predicted just from the lowest threshold parameters. Also, it is clear from Ref. [25] that the difference in the  $^1S_0$  and  $^3S_1$  phase shifts comes from difference of the singlet and triplet scattering lengths while the effective interactions are similar in the two channels. The realization of the Wigner symmetry does not arise from the size of the scattering length but rather from the long-distance properties of the effective interactions. In Ref. [31], the origin of the Wigner symmetry is unveiled in the framework of pionless effective field theory at leading order, but no mention is made concerning what happens when pion exchange interactions and the tensor coupling are included.

The purpose of the present paper is to outline under what conditions can these long distance symmetries be displayed. We will show that this is indeed the case and, moreover, for the SRG cutoff of about 600 MeV an extremely accurate fulfillment of Wigner SU(4) symmetry is found. By taking into account that in the SRG we are at any rate preserving phase

equivalence this result actually suggests a representation of the interaction based explicitly on the symmetry. This of course will have some implications for nuclear structure and nuclear reactions which deserve further study.

The paper is organized as follows. In Sec. II we review the SRG approach and provide the definition of a long-distance symmetry within such a framework. One good way to unveil a symmetry is to construct a set of sum rules where the symmetry is linearly broken. This is done in Sec. III. In Sec. IV we show our numerical methods and the corresponding results. Finally, in Sec. V we present our main conclusions and outlook for further work. In Appendix A we review the meaning of both the Wigner and Serber symmetries within the  $NN$  context. In Appendix B we analyze a fixed-point solution of the SRG equations and its stability properties.

## II. SRG AND SYMMETRIES

The formulation of the SRG is well known [10,32,33]. However, the equations are rather complicated (being integro-differential nonlinear coupled equations) and hence very few general properties have so far been deduced, so much insight is provided by numerical calculations or the study of simplified models. A textbook presentation is available [34] and a rigorous discussion has been carried out only recently [35] although the interesting case of unbounded operators which is the standard situation in nuclear physics has been left out. Therefore much understanding of these equations relies on numerical approaches and the use of a discretized momentum-space basis on a finite Hilbert space (see however [9,36] for some analytical models). The continuum limit will be analyzed in some detail in Appendix B.

The SRG makes a transformation which actually drives the system into a diagonal basis, suppressing exponentially off-diagonal elements, as we review here. Let us consider the evolution equation at the operator level in the SRG approach induced by the unitary transformation  $H_s = U_s H_0 U_s^\dagger$  with  $\eta(s) = \frac{dU_s}{ds} U_s^\dagger$ ,

$$\frac{dH_s}{ds} = [\eta_s, H_s], \quad (1)$$

with the anti-Hermitian generator  $\eta_s = [G_s, H_s]$ , where  $G_s$  is the SRG Hermitian generator which will be specified shortly. If  $H_{s=0} = H$  is the initial Hamiltonian one can easily see that when  $[G_s, H_s] = 0$  then the SRG equation has a stationary point. Conversely, stationary points of the SRG equation fulfill  $[[G_s, H_s], H_s] = 0$ . This means that the invariant subspaces of  $H_s$  eigenvectors are also invariant subspaces of  $G_s$ , whence a band-diagonal structure follows. Due to the commutator character of the equations one has an infinite set of conservation laws. Indeed, using the cyclic property of the trace we get

$$\frac{d}{ds} \text{Tr}(H_s^n) = n \text{Tr} \left( H_s^{n-1} \frac{dH_s}{ds} \right) = n \text{Tr} (H_s^{n-1} [\eta_s, H_s]) = 0. \quad (2)$$

In this paper we will use as initially suggested by Glazek and Wilson [6,7] the kinetic energy as the SRG generator,  $G_s = T$ . Using  $H_s = T + V_s$  we get for the potential energy

the evolution equation

$$\frac{dV_s}{ds} = [[T, V_s], V_s]. \quad (3)$$

For this choice one has that for any  $n$  and  $s$

$$\frac{d}{ds} \text{Tr}(V_s^n) = 0. \quad (4)$$

In Appendix B we will also show that the diagonal matrix elements of the standard scattering reaction  $R$  matrix is a stationary point of the previous equation when the potential is diagonal.

More generally, for an arbitrary operator  $O$  we get the equation

$$\frac{dO_s}{ds} = [[T, V_s], O_s]. \quad (5)$$

The purpose of the present paper is to outline under what conditions can the so-called long-distance symmetries be analyzed. In particular, for a symmetry group generator  $X$  we have

$$\frac{dX_s}{ds} = [[T, V_s], X_s]. \quad (6)$$

A symmetry at a given scale  $s$  must commute with both kinetic and potential energy operators and thus fulfills  $[X_s, T] = 0$  and  $[X_s, V_s] = 0$ . Using Jacobi's identity  $[[A, B], C] + [[C, A], B] + [[B, C], A] = 0$  we get

$$\frac{dX_s}{ds} = -[[X_s, T], V_s] - [[V_s, X_s], T] = 0. \quad (7)$$

A standard symmetry corresponds to a vanishing of the left-hand side, whereas a long-distance symmetry is a fixed point of the evolution along the similarity renormalization group at a given point. We will see that such a symmetry pattern appears within the SRG in regard to Wigner and Serber symmetries (see Appendix A for a short description). The variable  $s$  has dimensions of energy<sup>-2</sup> and it is customary to introduce the SRG cutoff  $\lambda = s^{-1/4}$ , which has dimensions of momentum.

As we have already mentioned, the previous manipulations are fully justified in a finite Hilbert space and typically correspond to a discretized momentum-space basis. The discretization effects are enhanced as the running Hamiltonian is driven toward the diagonal form. So one expects to evolve to a scale where the high-energy components are decoupled from the dynamics but also where the discretization effects are also unimportant. A feature of the SRG is that much of the SRG scale evolution happens already at the beginning and slows down as one approaches the scales of interest in nuclear applications.

We expect the long-distance symmetry to occur (if at all) at a given SRG scale, but this may depend on the SRG generator. For definiteness, we use here the SRG equations with the kinetic energy as the generator, which have  $T|\vec{p}\rangle = E_p|\vec{p}\rangle$  with  $E_p = p^2/M$ . In momentum space the equations read

$$\begin{aligned} & \frac{dV_s(\vec{p}', \vec{p})}{ds} \\ &= -(E_p - E'_p)^2 V_s(\vec{p}', \vec{p}) \\ &+ \int \frac{d^3q}{(2\pi)^3} (E_p + E_{p'} - 2E_q) V_s(\vec{p}', \vec{q}) V_s(\vec{q}, \vec{p}). \end{aligned} \quad (8)$$

Note that if we take zero momentum states

$$\frac{dV_s(\vec{0}, \vec{0})}{ds} = -2 \int \frac{d^3q}{(2\pi)^3} E_q \langle \vec{q} | V_s V_s^\dagger | \vec{q} \rangle \leq 0, \quad (9)$$

which means that zero-momentum matrix elements of the SRG-evolved potentials always decrease. Note that this does not prevent the momentum from becoming infinite at some finite value of  $s$ . The conservation of  $\text{Tr}(V_s^n)$  means that the zero-momentum strength increases at the cost of depleting the high- and off-diagonal matrix elements.

### III. SYMMETRIES AND PARTIAL WAVE DECOMPOSITION

#### A. Kinematical symmetries

The most general self-adjoint interaction in momentum space which is invariant under parity, time-reversal, isospin, and Galilean invariance has the following form [37]:

$$\begin{aligned} V(\vec{p}', \vec{p}) = & V_C + \vec{\tau}_1 \cdot \vec{\tau}_2 W_C + (V_S + \vec{\tau}_1 \cdot \vec{\tau}_2 W_S) \vec{\sigma}_1 \cdot \vec{\sigma}_2 \\ & + (V_{LS} + \vec{\tau}_1 \cdot \vec{\tau}_2 W_{LS}) i(\vec{\sigma}_1 + \vec{\sigma}_2) \cdot (\vec{p}' \times \vec{p}) \\ & + (V_T + \vec{\tau}_1 \cdot \vec{\tau}_2 W_T) S_{12}(\vec{p}' - \vec{p}) \\ & + (V_Q + \vec{\tau}_1 \cdot \vec{\tau}_2 W_Q) S_{12}(\vec{p}' \times \vec{p}) \\ & + (V_P + \vec{\tau}_1 \cdot \vec{\tau}_2 W_P) S_{12}(\vec{p}' + \vec{p}), \end{aligned}$$

where the tensor operator is defined as

$$S_{12}(\vec{q}) = [\vec{\sigma}_1 \cdot \vec{q} \vec{\sigma}_2 \cdot \vec{q} - \frac{1}{3} q^2 \vec{\sigma}_1 \cdot \vec{\sigma}_2], \quad (10)$$

and  $\vec{\sigma}_i$  and  $\vec{\tau}_i$  are the Pauli matrix spin and isospin operators for the  $i$ th particle respectively. The subscripts refer to the central ( $C$ ), spin-spin ( $S$ ), tensor ( $T$ ), spin-orbit ( $SL$ ), quadratic spin-orbit ( $Q$ ), and quadratic-velocity-dependent ( $P$ ) components of the  $NN$  interaction, each of which occurs in an isoscalar ( $V$ ) and an isovector ( $W$ ) version. Here  $\vec{\sigma}_{1,2}$  and  $\vec{\tau}_{1,2}$  are the usual spin and isospin operators of the two nucleons. Note that the so-defined condition of zero angular averaging for the tensor operator  $\int d^2\hat{p} S_{12}(\vec{p}) = 0$  is fulfilled and, as a consequence, our results will be stated in a rather simple form. Note also that the central parts can be deduced by tracing the potential in the spin-isospin space after appropriate multiplication of the operators  $\mathbf{1}$ ,  $\mathbf{S}_i$ ,  $\mathbf{T}_a$ , and  $\mathbf{G}_{ia}$  (see Appendix A).

An advantage of using the momentum-space basis is that the generalized Pauli principle can be incorporated directly into the potential which is antisymmetric under the exchange of the final states, which in the center-of mass (CM) frame reads

$$V_{1',2';1,2}(\vec{p}', \vec{p}) = -V_{2',1';1,2}(-\vec{p}', \vec{p}), \quad (11)$$

where the indices represent a full Pauli spinor-isospinor state. These kinematical symmetries are preserved by the SRG equations. This means that if we have a starting potential  $V(\vec{p}', \vec{p})$  which evolves into  $V_s(\vec{p}', \vec{p})$  then  $V(R\vec{p}', R\vec{p})$  evolves into  $V_s(R\vec{p}', R\vec{p})$ . In particular, a potential remains rotational invariant along the SRG evolution and the general form is maintained throughout the evolution. This of course includes the generalized Pauli principle (11).

### B. Long-distance symmetries

The off-shell  $T$  matrix has the same decomposition as for the potential and hence contains 12 independent amplitudes, but on-shell, because of the condition  $|\vec{p}'| = |\vec{p}|$ , one just gets 10 different amplitudes since one has the identity  $\sigma_1 \cdot \sigma_2 = \sigma_1 \cdot \hat{n}\sigma_2 \cdot \hat{n} + \sigma_1 \cdot \hat{m}\sigma_2 \cdot \hat{m} + \sigma_1 \cdot \hat{l}\sigma_2 \cdot \hat{l}$ , where  $\hat{n}$ ,  $\hat{m}$ ,  $\hat{l}$  are three orthonormal vectors in three-dimensional space such as those proportional to  $\vec{p}' - \vec{p}$ ,  $\vec{p}' + \vec{p}$ , and  $\vec{p}' \times \vec{p}$ .

Following the description in Ref. [38] (see also [39,40]) one can undertake the projection onto partial waves. The nonlinear SRG equation can be simplified by using conservation of angular momentum. If we just define for a given spin the standard partial wave decomposition

$$\langle \vec{p}' | V_\lambda^S | \vec{p} \rangle = N \sum_{JMLL'} \mathcal{Y}_{LS}^{JM}(\hat{p}') V_{LL'}^{JS}(p', p) \mathcal{Y}_{L'S}^{JM\dagger}(\hat{p}), \quad (12)$$

with  $N = 4\pi^2/M$ , we get an infinite set of coupled equations with good total angular momentum. The three-dimensional structure contains central and noncentral forces. Inserting this into the SRG equation we get the coupled-channel equations

$$\begin{aligned} & \frac{dV_s(p, p')}{ds} \\ &= -(p^2 - p'^2)^2 V_s(p, p') \\ &+ \frac{2}{\pi} \int_0^\infty dq q^2 (p^2 + p'^2 - 2q^2) V_s(p, q) V_s(q, p'), \end{aligned} \quad (13)$$

where  $V_s(p, p')$  is used as a brief notation for the projected  $NN$  potential matrix elements,

$$V_s^{(JLL'S:I)}(p, p') = \langle p(LS)J; I | V_s | p'(L'S)J; I \rangle, \quad (14)$$

in a partial-wave relative momentum-space basis,  $|q(LS)J; I\rangle$ , with normalization such that

$$1 = \frac{2}{\pi} \int_0^\infty dq q^2 |q(LS)J; I\rangle \langle q(LS)J; I|. \quad (15)$$

The superscripts  $J$ ,  $L(L')$ ,  $S$ , and  $I$  denote, respectively, the total angular momentum, the orbital angular momentum, the spin, and the isospin quantum numbers of the  $NN$  state. For noncoupled channels ( $L = L' = J$ ), the matrix elements  $V_s(p, p')$  are simply given by  $V_s(p, p') \equiv V_s^{(JJJS:I)}(p, p')$ . For coupled channels ( $L, L' = J \pm 1$ ), the  $V_s(p, p')$  represent  $2 \times 2$  matrices of matrix elements for the different combinations of  $L$  and  $L'$ . The advantage of using the partial-wave decomposition is that every single channel may be evolved independently from a given initial solution,  $V_{s=0}(p', p)$ , to yield a unitarily equivalent potential

$$V_s(p', p) = \int dq q U_s(q', p')^* V_{s=0}(q', q) U_s(q, p). \quad (16)$$

A further property is that for low momenta we have the threshold behavior

$$V_s(p', p) = C_{L,L'}(s) p^L (p')^{L'} [1 + O(p^2, p'^2)], \quad (17)$$

which means also that the matrix  $C_{L,L'}(s)$  is a decreasing function of the SRG cutoff; i.e.,  $C'_{L,L'}(s)$  is negative definite.

### C. Perturbation theory

In the case of rotational invariance, the symmetry is preserved along the SRG trajectory. In the case of a long-distance symmetry the symmetry breaking strength depends on the SRG scale. Let us thus consider the expansion around the central solution; i.e., let us split

$$\mathcal{V}_{NN} = V_0 + V_1, \quad (18)$$

where  $[\vec{L}, V_0] = 0$  whereas  $[\vec{J}, V_1] = 0$  and  $[\vec{L}, V_1] \neq 0$ . The zeroth-order potential commutes with  $L, S, T$  and so the corresponding potential may be denoted as  $V_L^{ST}$ . The total potential commutes with the total angular momentum  $J = L + S$  and  $S^2$ . Of course the goodness of this separation depends on the SRG scale  $\lambda$ , but we expect it to work better the lower the scale. Inserting the decomposition (18) into the SRG equation we have the zeroth-order equation

$$\begin{aligned} & \frac{dV_s^{(0)}(\vec{p}', \vec{p})}{ds} \\ &= -(E_p - E_{p'})^2 V_s^{(0)}(\vec{p}', \vec{p}) \\ &+ \int \frac{d^3q}{(2\pi)^3} (E_p + E_{p'} - 2E_q) V_s^{(0)}(\vec{p}', \vec{q}) V_s^{(0)}(\vec{q}, \vec{p}), \end{aligned} \quad (19)$$

whereas the first-order equation is

$$\begin{aligned} & \frac{dV_s^{(1)}(\vec{p}', \vec{p})}{ds} \\ &= -(E_p - E_{p'})^2 V_s^{(1)}(\vec{p}', \vec{p}) + \int \frac{d^3q}{(2\pi)^3} (E_p + E_{p'} - 2E_q) \\ &\quad \times [V_s^{(1)}(\vec{p}', \vec{q}) V_s^{(0)}(\vec{q}, \vec{p}) + V_s^{(0)}(\vec{p}', \vec{q}) V_s^{(1)}(\vec{q}, \vec{p})]. \end{aligned} \quad (20)$$

Clearly, because  $V_0$  is central we get that the linear combinations are preserved as long as the noncentral contribution remains a small correction. Generally, we do not expect it to be the case, particularly not for the initial potential.

### D. Sum rules

Rather than analyzing the evolution of the generators we prefer to check the running of a set of sum rules based on first-order perturbation theory in noncentral components of the potential, which helped to disentangle some correlations in  $NN$  fits [41,42] and have been shown to work well at the level of phase shifts and  $V_{\text{lowk}}$  potentials in Refs. [25,26]. The main idea is to decompose the potential into central and noncentral pieces, as in Eq. (18), and assume the noncentral piece to be of the form

$$V_1 = L \cdot S V_{LS} + S_{12} V_T. \quad (21)$$

One property fulfilled by the noncentral interaction is that the trace in spin-isospin space vanishes. This suggests a set of sum rules at the partial wave level. Using first-order perturbation theory [25,26] we deduce the following linear combinations



for triplet  $P$  waves:

$$V_{3P_C} = \frac{1}{9}(V_{3P_0} + 3V_{3P_1} + 5V_{3P_2}), \quad (22)$$

$$V_{3P_T} = -\frac{5}{72}(2V_{3P_0} - 3V_{3P_1} + V_{3P_2}), \quad (23)$$

$$V_{3P_{LS}} = -\frac{1}{12}(2V_{3P_0} + 3V_{3P_1} - 5V_{3P_2}); \quad (24)$$

for triplet  $D$  waves we have

$$V_{3D_C} = \frac{1}{15}(3V_{3D_1} + 5V_{3D_2} + 7V_{3D_3}), \quad (25)$$

$$V_{3D_T} = -\frac{7}{120}(3V_{3D_1} - 5V_{3D_2} + 2V_{3D_3}), \quad (26)$$

$$V_{3D_{LS}} = -\frac{1}{60}(9V_{3D_1} + 5V_{3D_2} - 14V_{3D_3}); \quad (27)$$

for triplet  $F$  waves we have

$$V_{3F_C} = \frac{1}{21}(5V_{3F_2} + 7V_{3F_3} + 9V_{3F_4}), \quad (28)$$

$$V_{3F_T} = -\frac{5}{112}(4V_{3F_2} - 7V_{3F_3} + 3V_{3F_4}), \quad (29)$$

$$V_{3F_{LS}} = -\frac{1}{168}(20V_{3F_2} + 7V_{3F_3} - 27V_{3F_4}); \quad (30)$$

and for triplet  $G$  waves we have

$$V_{3G_C} = \frac{1}{27}(7V_{3G_3} + 9V_{3G_4} + 11V_{3G_5}), \quad (31)$$

$$V_{3G_T} = -\frac{77}{2160}(5V_{3G_3} - 9V_{3G_4} + 4V_{3G_5}), \quad (32)$$

$$V_{3G_{LS}} = \frac{1}{360}(-35V_{3G_3} - 9V_{3G_4} + 44V_{3G_5}). \quad (33)$$

In terms of the previous definitions Serber symmetry reads

$$0 = V_{3P_C} = V_{3F_C} = V_{3H_C} = \dots, \quad (34)$$

whereas Wigner symmetry implies

$$V_{1S_0} = V_{3S_C}, \quad V_{1D_2} = V_{3D_C}, \quad V_{1G_4} = V_{3G_C}. \quad (35)$$

#### IV. NUMERICAL RESULTS

Here we provide some details on the numerical evolution. In order to solve the Wegner's flow equation, we discretize the momentum space using a Gaussian grid of  $N$  mesh points. This leads us to a system of  $N^2$  nonlinear coupled first-order differential equations. The system can then be solved with an implementation of a fifth-order Runge-Kutta algorithm with adaptive step. In this work we use  $N = 200$  points.

Since the potentials we are evolving through the SRG are all regular, we set an ultraviolet cutoff at  $\Lambda = 30 \text{ fm}^{-1}$ , which is beyond the point where regulated potentials vanish. In principle, one could take a larger cutoff value provided the number of points in the grid are enough to ensure the convergence of the Runge-Kutta algorithm. If the cutoff is too large, one needs too many points in the grid and the number of coupled equation becomes too large to be solved in a reasonable time.

We illustrate our points for the Argonne AV18 potential [43], which fits not only the  $NN$  phase shifts of the Nijmegen data base PWA [46] but also the deuteron elastic form factors and has been used quite often successfully for nuclear structure calculations [3]. The diagonal matrix elements  $V(p, p)$  and fully off-diagonal matrix elements  $V(p, 0)$  are depicted in Figs. 1 and 2, respectively. We compare the initial potentials and the SRG potentials evolved to  $\lambda = 2 \text{ fm}^{-1}$  and  $\lambda = 1 \text{ fm}^{-1}$ . As we see, already above  $\lambda = 2 \text{ fm}^{-1}$  the potentials for

the  $^1S_0$  and  $^3S_1$  waves cross. This is an indication that Wigner symmetry works very well around that scale. This trend is also observed in even partial waves such as  $D$  and  $G$ , where the effect of SRG evolution becomes less important as the angular momentum is increased. On the other hand, odd partial waves provide hints of the Serber symmetry as one sees that the  $^1L$  potential is much larger than the  $^3L_C$  combination.

A comparison between the Argonne AV18 potential [43], the Nijmegen II potential [44], and the chiral next-to-next-to-leading order (N3LO) potential of Entem and Machleidt [45] is presented in Fig. 3 for the similarity cutoff  $\lambda = 2 \text{ fm}^{-1}$  and for the  $S$  and  $P$  waves. As we see, there is some degree of universality, as one might expect since these potentials are phase equivalent, although the strength is distributed differently, particularly in the N3LO chiral potential case.

As we see, the potential for the  $^3S_1$  wave changes rather dramatically when going from  $\lambda = 2$  to  $1 \text{ fm}^{-1}$ , in contrast to the other waves where apparently a much more stable result is obtained. This feature is due to the use of the simple generator  $\eta_s = [T, H_s]$ , where  $T$  is the kinetic energy. In Wegner's original formulation [8] the generator  $\eta = [D_s, H_s]$  was used, where  $D_s$  is the diagonal part of  $H_s$ . Actually, as shown by Glazek and Perry [13] the generator  $\eta_s = [T, H_s]$  can produce divergencies in theories with bound states, as in the case of the  $NN$  interaction in the  $^3S_1$ - $^3D_1$  channel, limiting how far the transformation can be run. When the SRG cutoff  $\lambda = 1/s^{\frac{1}{4}}$  approaches the momentum scale at which a bound state emerges, the strength of the SRG-evolved interactions increases significantly. This occurs because the transformation tends to move the bound-state eigenvalue to the low-momentum part of the Hamiltonian's diagonal, forcing the interaction to grow in order to maintain the bound state at the right value. In the Appendix B we show that actually in the limit  $\lambda \rightarrow 0$  the SRG equation becomes stationary when the SRG potential becomes the reaction matrix, which in the single-channel case becomes

$$\lim_{\lambda \rightarrow 0} V_\lambda(p, p) = -\frac{\tan \delta(p)}{p}, \quad (36)$$

and a similar equation is obtained in the coupled-channel case. Note that this diverges when the phase shift goes through  $90^\circ$ , a situation which only occurs for the  $^3S_1$  channel for  $p \sim 100 \text{ MeV}$ . On the other hand, there is no divergence problem when using Wegner's generator  $\eta = [D_s, H_s]$ , because the bound-state eigenvalue is kept at the natural momentum scale as the SRG cutoff is lowered, suggesting that actually the generator initially proposed by Wegner has better infrared properties. In this sense it would be interesting to check the present results for the Wegner flow case. The advantages of other SRG generators have been considered recently [47].

Finally, we can fine tune the SRG cutoff so that we obtain the best possible fulfillment of the Wigner symmetry, which is slightly above  $\lambda$ . We call this  $\lambda_{\text{Wigner}}$ . This, of course, would have far-reaching consequences for the analysis of finite nuclei on the basis of symmetry.

Our results for the  $S$  waves are presented in Fig. 4 where the similarity cutoff runs from 5 to  $2 \text{ fm}^{-1}$ . We can see that both  $S$  waves evolve in the same direction, becoming more

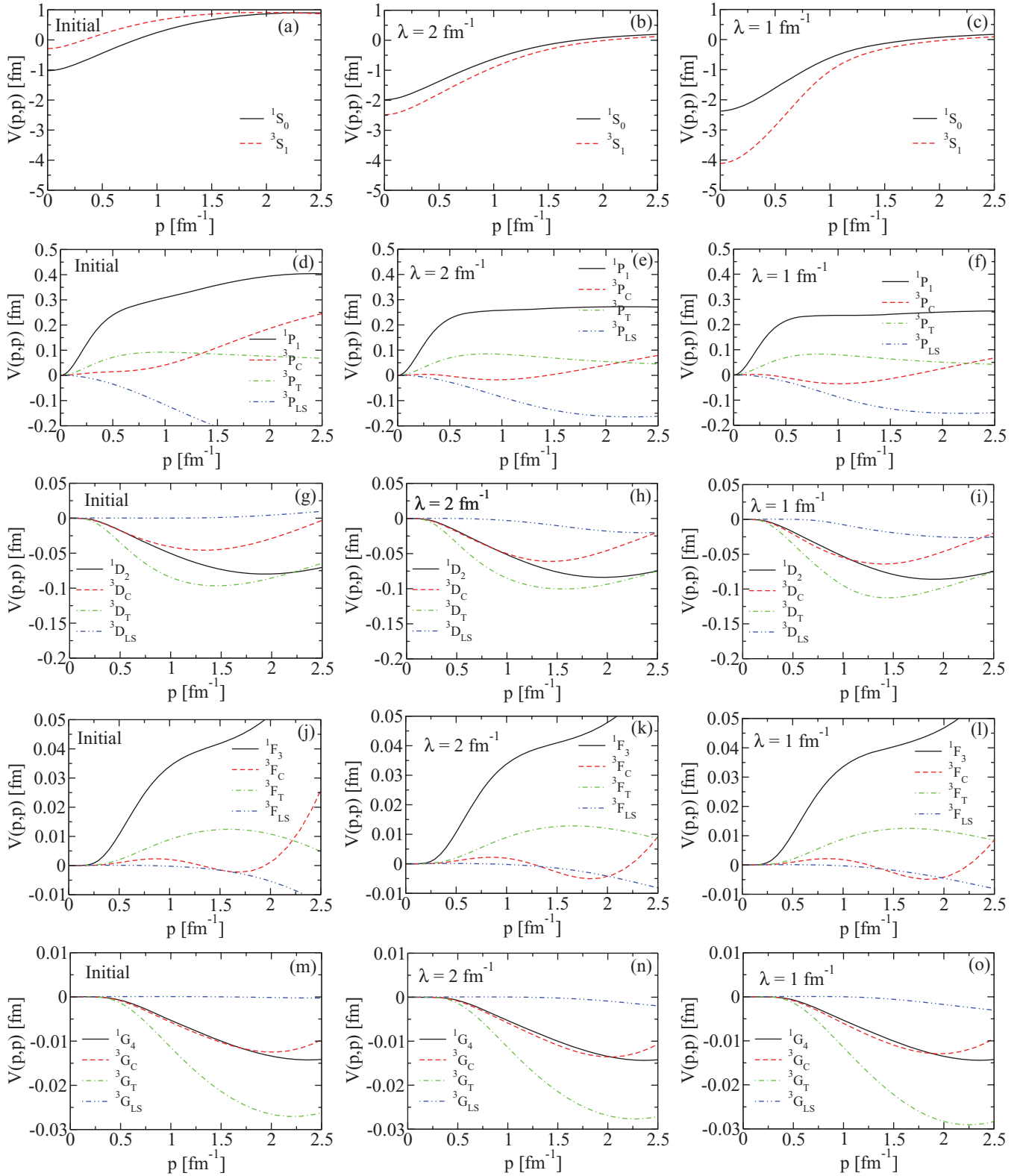


FIG. 1. (Color online) Diagonal matrix elements of the SRG-evolved Argonne AV18 potential [43]  $V(p, p)$  (in fm) as a function of the CM momentum (in  $\text{fm}^{-1}$ ) for the  $S$ ,  $P$ ,  $D$ ,  $F$ , and  $G$  partial-wave components for different values of the similarity cutoff  $\lambda$ . Left panel: Initial potential ( $\lambda = \infty$ ). Central panel:  $\lambda = 2 \text{ fm}^{-1}$ . Right panel:  $\lambda = 1 \text{ fm}^{-1}$ .

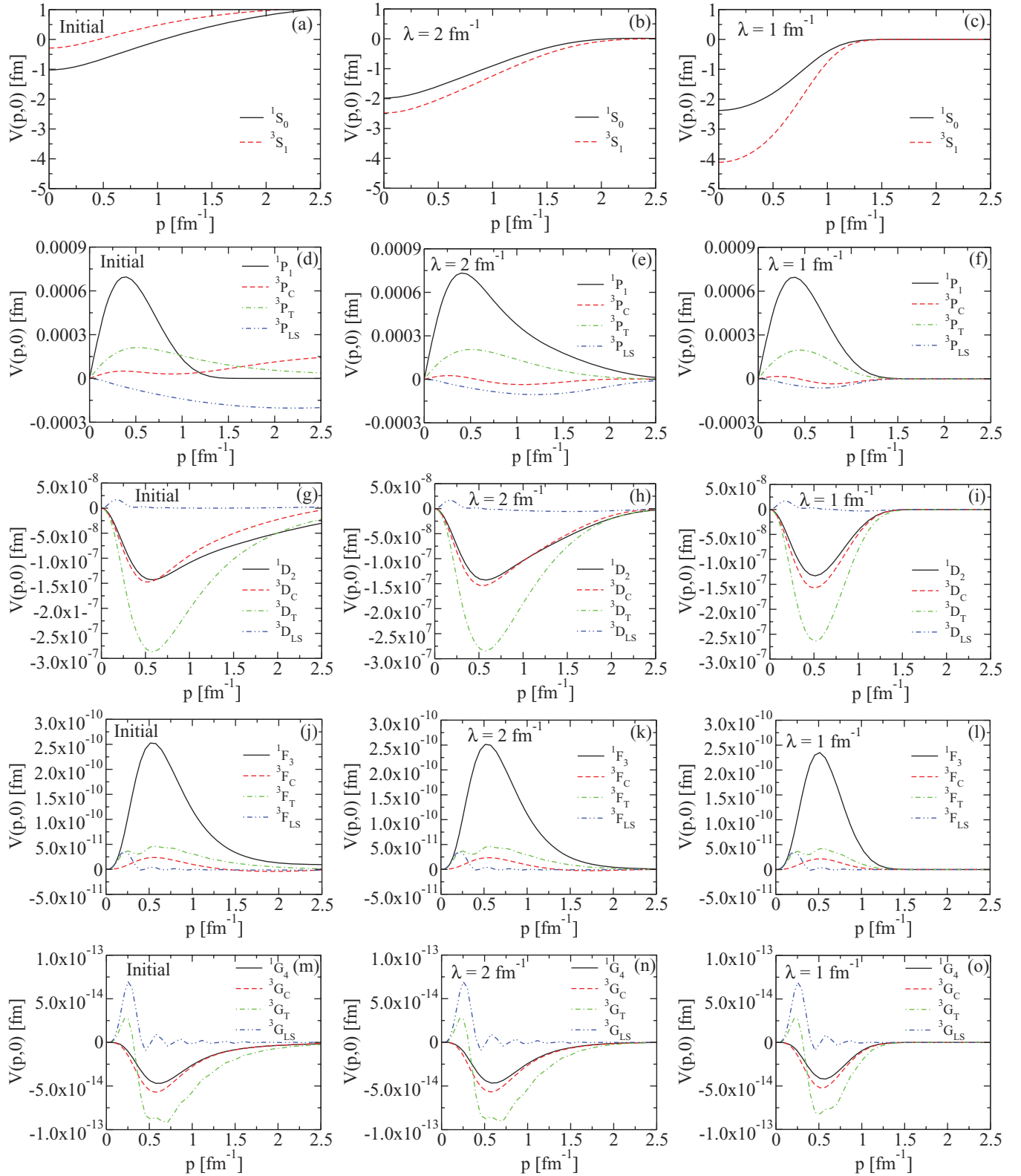


FIG. 2. (Color online) Fully off-diagonal matrix elements of the SRG-evolved Argonne AV18 potential [43] (in fm) as a function of the CM momentum (in  $\text{fm}^{-1}$ ) for the  $S$ ,  $P$ ,  $D$ ,  $F$ , and  $G$  partial-wave components for different values of the similarity cutoff  $\lambda$ . Left panel: Initial potential ( $\lambda = \infty$ ). Central panel:  $\lambda = 2 \text{ fm}^{-1}$ . Right panel:  $\lambda = 1 \text{ fm}^{-1}$ .

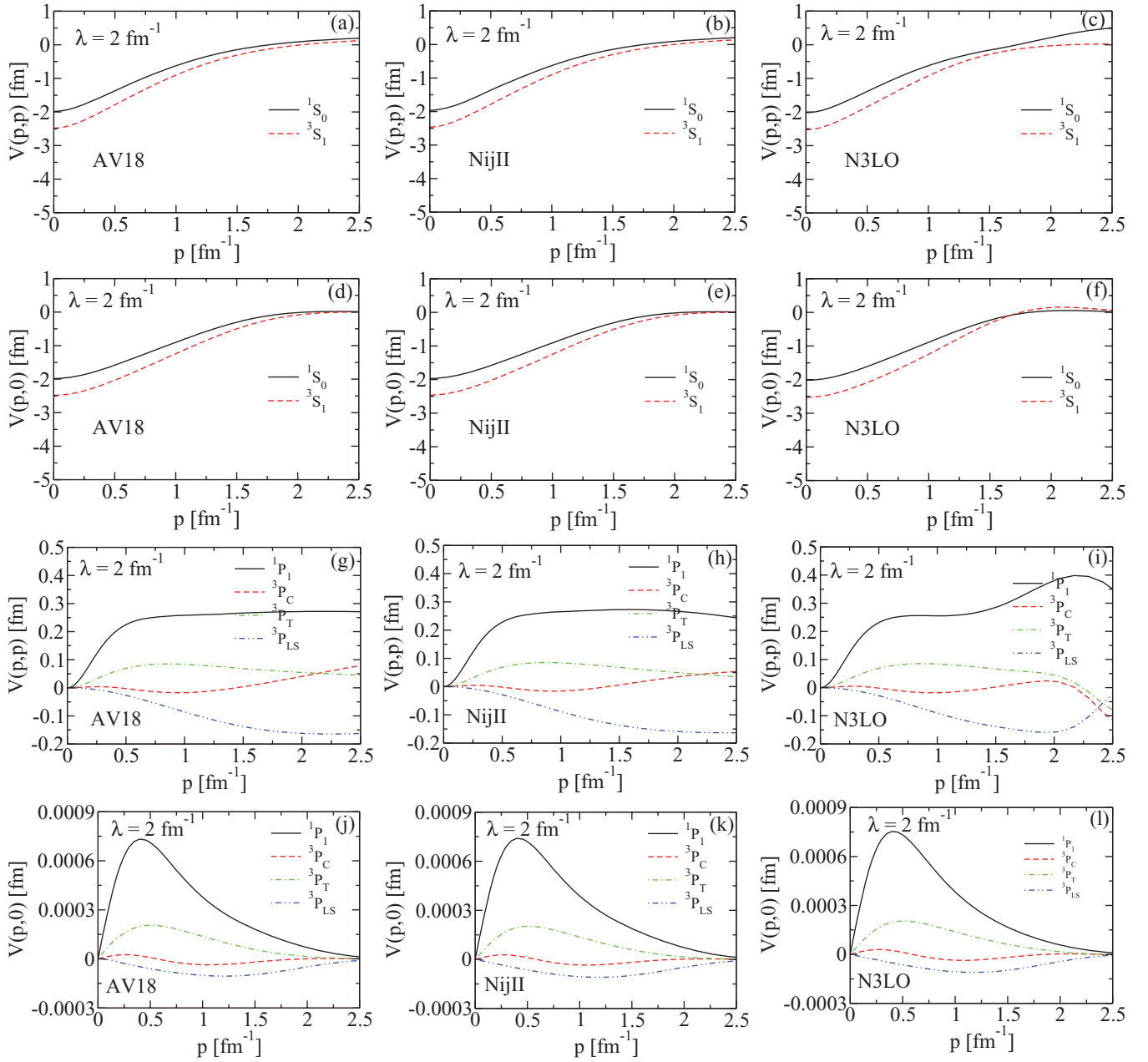


FIG. 3. (Color online) Comparison between the diagonal  $V(p, p)$  and fully off-diagonal  $V(p, 0)$  matrix elements of the SRG-evolved potentials for the  $S$  and  $P$  waves as a function of the CM momentum  $p$  (in  $\text{fm}^{-1}$ ) for a similarity cutoff  $\lambda = 2 \text{ fm}^{-1}$ . Left panels: Argonne AV18 potential [43]. Central panels: Nijmegen II potential [44]. Right panels: Chiral N3LO potential of Entem and Machleidt [45].

attractive. At  $\lambda_{\text{Wigner}} = 3 \text{ fm}^{-1}$ , the SRG-evolved interaction in the two  $S$  waves are practically identical and for  $\lambda = 2 \text{ fm}^{-1}$  the evolved potential in the triplet channel is stronger than in the singlet case. As expected, the evolution in the triplet state is faster than in the singlet state. The deuteron pole is at an imaginary momentum scale  $p_d \sim i0.23 \text{ fm}^{-1}$  while the pole corresponding to the  ${}^1S_0$  virtual bound state is at a much smaller momentum scale  $p_v \sim i0.04 \text{ fm}^{-1}$ . Thus, when evolving to similarity cutoffs in the range we are considering, the enhancement in the strength of the interaction that comes from using the simple generator  $\eta = [T, H(s)]$  is sensible only in the  ${}^3S_1$  channel. As we see, at  $\lambda_{\text{Wigner}}$  the agreement between

the  ${}^3S_1$  and  ${}^1S_0$  SRG-evolved interactions is indeed remarkable for both the diagonal and the fully off-diagonal elements. It is important to note that the difference between the  ${}^1S_0$  and the  ${}^3S_1$  phase shifts evaluated from the initial unevolved potentials is reproduced at any rate through the SRG evolution, since the unitary SRG transformation changes the interactions (independently in each partial-wave channel) while preserving the corresponding phase shifts.

For the  $D$  waves the results are displayed in Fig. 5, where we can see that generally for  $p', p < 0.7 \text{ fm}^{-1}$  Wigner symmetry is well fulfilled. Note that the better fulfillment of the Wigner symmetry for slightly large values of  $p$  occurs for a similarity



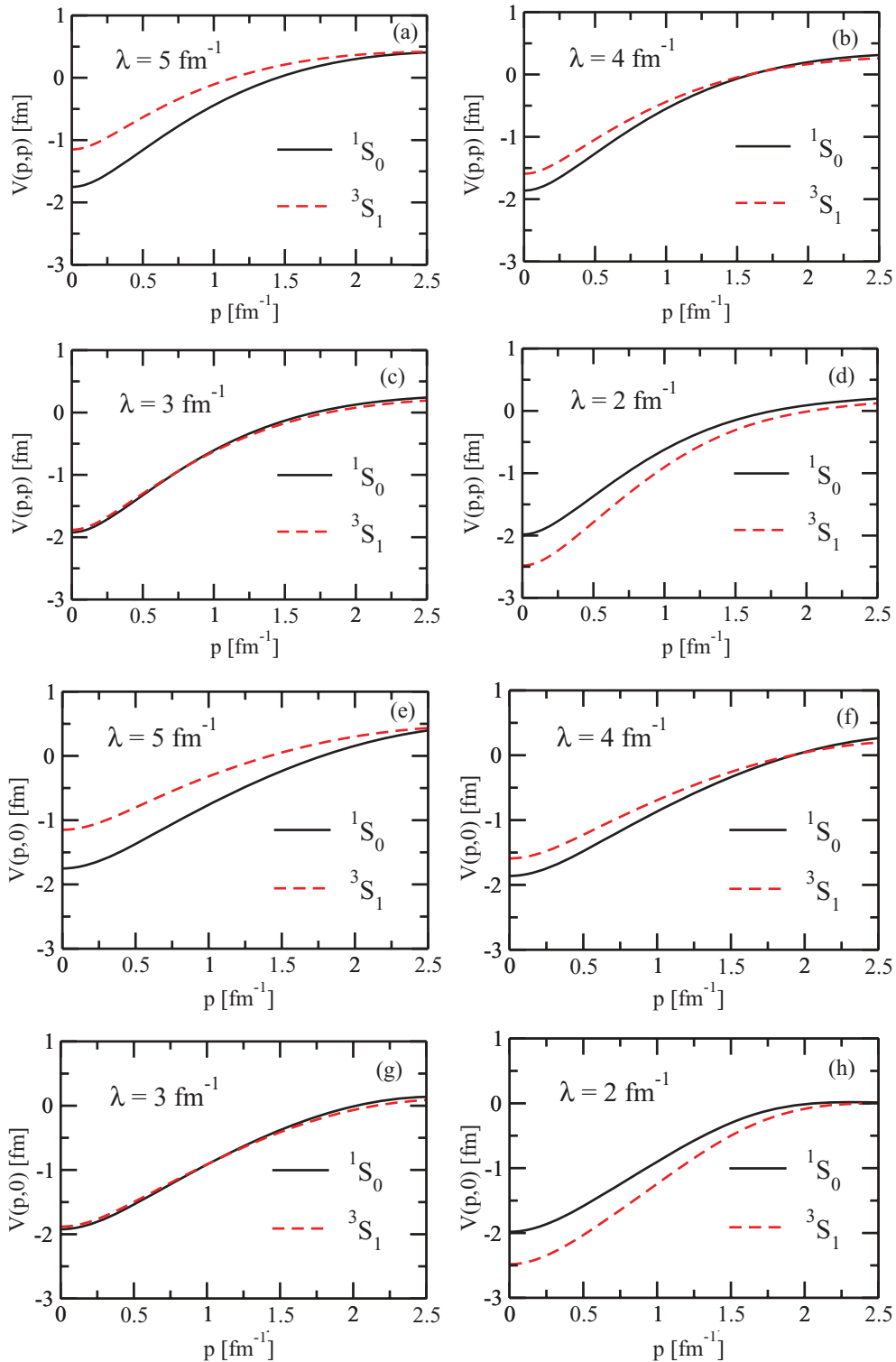


FIG. 4. (Color online) Comparison between diagonal,  $V(p, p)$ , and fully off-diagonal,  $V(p, 0)$ , matrix elements of the SRG-evolved potentials for the  $S$  waves (in fm) as a function of the CM momentum  $p$  (in  $\text{fm}^{-1}$ ), showing that the Wigner similarity cutoff is  $\lambda_{\text{Wigner}} \approx 3 \text{ fm}^{-1}$ . We use the Argonne AV18 potential as the initial condition [43].

cutoff of  $2 \text{ fm}^{-1}$ . A somewhat similar situation occurs also for  $G$  waves, as shown in Fig. 6, where now a better fulfillment of the Wigner symmetry exists for a similarity cutoff of  $4 \text{ fm}^{-1}$ . It is interesting to note that the value of the similarity cutoff where

we have the better fulfillment of the Wigner symmetry is not unique, being different in each of the even angular momentum waves we considered. Of course, while we do not expect *a priori* an exact fulfillment of  $SU(4)$  spin-isospin symmetry it

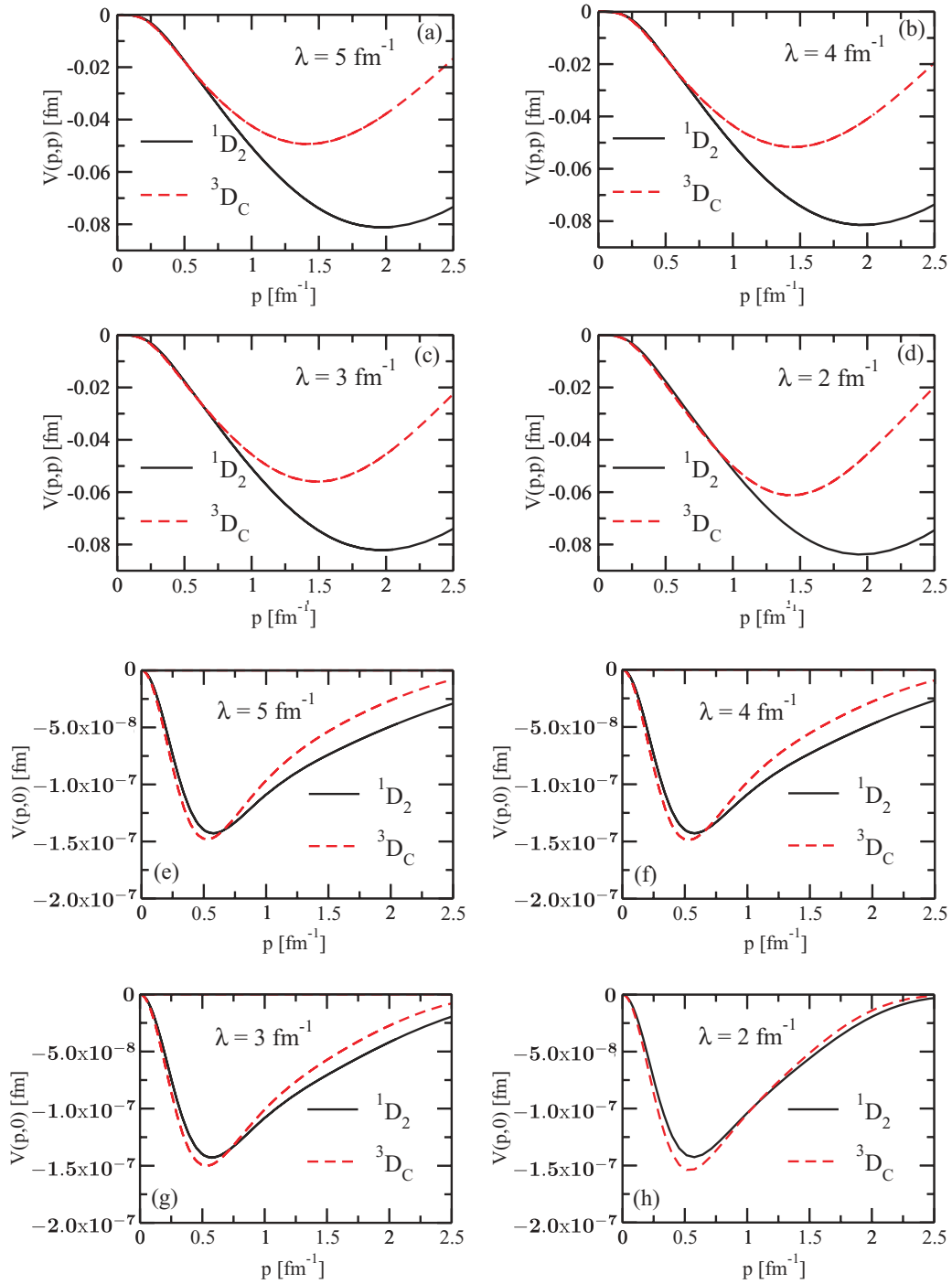


FIG. 5. (Color online) Comparison between diagonal,  $V(p, p)$ , and fully off-diagonal,  $V(p, 0)$ , matrix elements of the SRG-evolved potentials for the  $D$  waves (in fm) as a function of the CM momentum  $p$  (in  $\text{fm}^{-1}$ ).

is remarkable how well it works by taking into account that high-quality potentials have not been designed to implement the symmetry by any means.

With the definitions of the potential we get the simple expressions

$$V_{LC} = 2\pi \int_{-1}^1 dz P_L(z) [V_C - 3V_S + \tau(W_C - 3W_S)], \quad (37)$$

$$V_{3LC} = 2\pi \int_{-1}^1 dz P_L(z) [V_C + V_S + \tau(W_C + W_S)], \quad (38)$$

where  $\tau = 4I - 3$ .

The nontriviality of the Serber symmetry is realized by noting that we just change the angle without changing the nucleons. To elaborate a bit further let us consider the standard

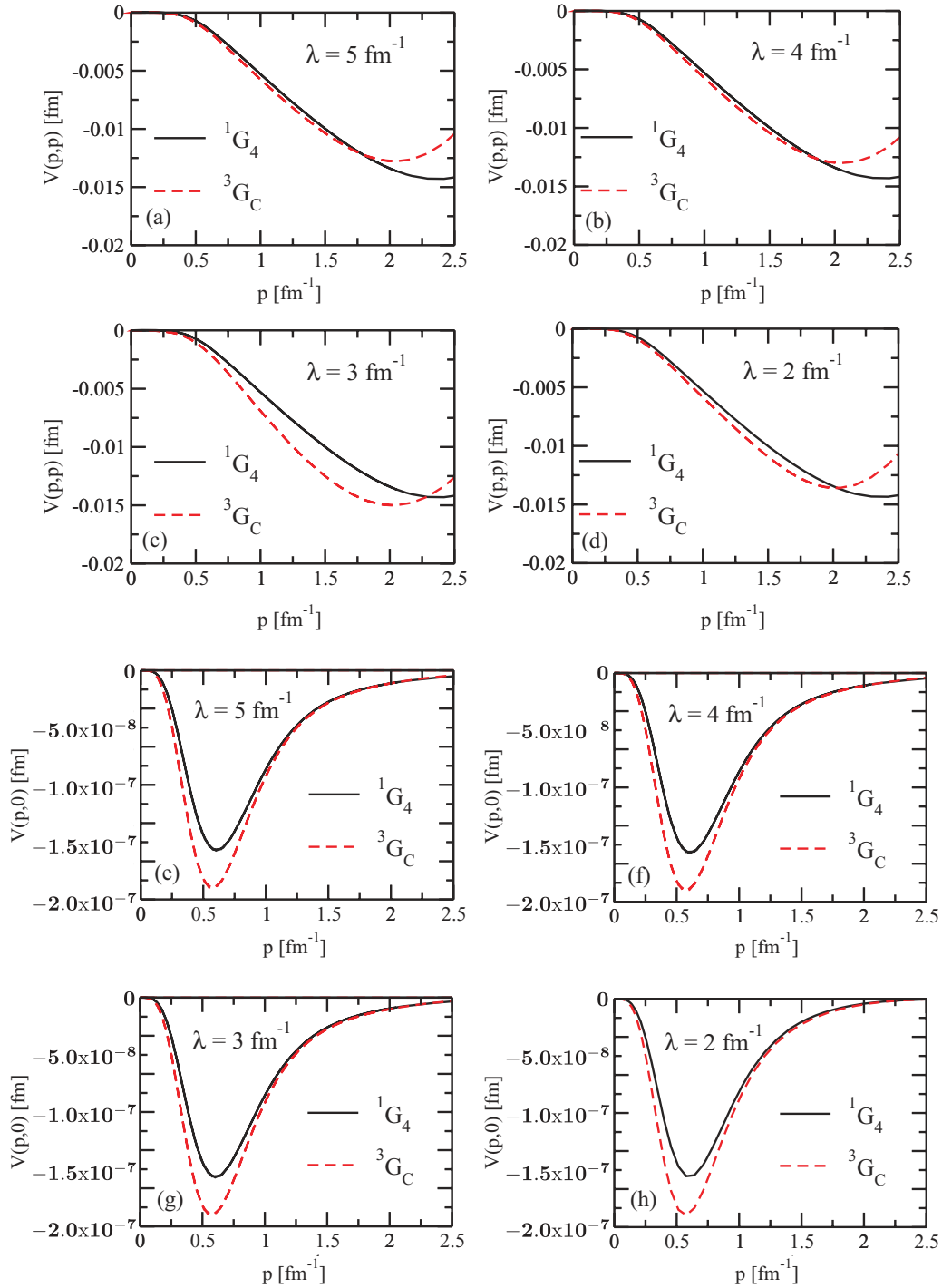


FIG. 6. (Color online) Comparison between diagonal,  $V(p, p)$ , and fully off-diagonal,  $V(p, 0)$ , matrix elements of the SRG-evolved potentials for the  $G$  waves (in fm) as a function of the CM momentum  $p$  (in  $\text{fm}^{-1}$ ).

Fierz identities. For the spin-isospin operators one gets

$$P_{1'2'}\mathbf{1} = \frac{1}{2}[\mathbf{1} + \sigma], \quad P_{1'2'}\sigma = \frac{1}{2}[\mathbf{1} - 3\sigma],$$

$$P_{1'2'}(\sigma_1 + \sigma_2) = -(\sigma_1 + \sigma_2), \quad P_{1'2'}(\sigma_1 + \sigma_2) = -(\sigma_1 + \sigma_2),$$

and similar equations for isospin operators. These identities imply that the following combinations of scalar functions are,

respectively, even or odd in  $z$ :

$$\begin{aligned} & [V_C - 3V_S + \tau(W_C - 3W_S)]|_{-z} \\ & = [V_C - 3V_S + \tau(W_C - 3W_S)]|_z, \\ & [V_C + V_S + \tau(W_C + W_S)]|_{-z} \\ & = -[V_C + V_S + \tau(W_C + W_S)]|_z. \end{aligned} \quad (39)$$

Therefore, the orbital parity of the integrand and the Legendre polynomial in Eqs. (37) and (38) are *the same* and do not suggest that any of them vanish. Instead, the symmetries imply

$$0 = V_C + V_S + W_C + W_S, \quad (40)$$

$$V_C - 3V_S + W_C - 3W_S = V_C + V_S - 3W_C - 3W_S.$$

We recall that the large- $N_c$  analysis of Ref. [29] yields  $V_C, W_S = O(N_c)$ , whereas  $W_C, V_S = O(N_c^{-1})$ , suggesting from QCD that Wigner symmetry holds [second line of Eq. (40)] in the even- $L$  partial waves, *exactly* as we find here for the SRG model. Note also that Serber symmetry under those conditions implies  $V_C + W_S = 0$ . These conclusions have been analyzed in great detail along several viewpoints [25–28] and are confirmed here within the SRG. In any case, our results suggest that it must be possible to impose these approximate symmetries to a  $NN$  potential from the very beginning.

## V. CONCLUSIONS AND OUTLOOK

In the present paper we have analyzed the concept of long-distance symmetries as applied to the similarity renormalization group. We have shown that very similarly to the case of the  $V_{\text{lowk}}$  formulation, the symmetry pattern of Wigner symmetry in partial waves with even angular momentum as well as the Serber symmetry in odd partial waves holds for the SRG cutoff around  $\lambda \sim 3 \text{ fm}^{-1}$ . This is somewhat remarkable since SRG only provides an exponential decoupling between low- and high-energy modes, bringing the effective interaction to the diagonal form, whereas  $V_{\text{lowk}}$  corresponds to integrate out high-energy components. It is also noteworthy that the symmetry arises at scales where in few-body calculations the induced three-body forces become small [18,19].

In this work we have not evolved the three-body force through the SRG, so that no statements on the three-body SU(4)-violating terms can be made, even knowing that in the two-body case the SU(4)-violating terms get small. From this point of view the extension of the present results to three- and four-body forces and the analysis of their symmetry structure would be of great interest.

The underlying symmetry pattern unveiled by our SRG analysis appears intriguing and unexpected from the modern viewpoint of coarse-graining high-quality interactions. From such a perspective this fits somewhat the vague concept of an accidental symmetry. Note that here we use the standard concept of accidental symmetry from quantum mechanics instead of the field theory one: a symmetry which is realized although not foreseen.

There is a long tradition on the phenomenological consequences of Wigner symmetry for the properties of nuclei and nuclear matter (for a review see, e.g., Ref. [48]). A recent work [49] analyzes the SU(4) pattern of pairing forces within a  $V_{\text{lowk}}$  framework, which quite naturally follow the symmetry pattern. Our results, in particular the existence of a SRG scale at which the Wigner symmetry becomes quite accurate, not only provide a natural explanation for this fact but suggest the pursuit of further studies in future work within the current SRG framework.

From a fundamental viewpoint, QCD large- $N_c$ -based arguments foresee fulfilling the symmetry with a relative  $O(1/N_c^2)$

accuracy, so one does not expect a perfect fulfillment of the Wigner symmetry. On the other hand, nowhere in the design and optimization of the modern high-quality interactions which have been successfully applied to the structure of finite nuclei was the Wigner symmetry pattern explicitly implemented. In this regard, the accuracy with which by choosing a suitable SRG scale the symmetry seems to hold suggests that this is a property of the data themselves which emerges when the interaction is resolved with a specific length scale and not so much of the original (bare) potentials used to fit the  $NN$  scattering database. Finally, one should recognize that while the use of symmetries for coarse-grained effective interactions is not mandatory we expect by explicit symmetry considerations additional simplifications of the complicated nuclear many-body problem. Work along these lines is in progress.

## ACKNOWLEDGMENTS

Computational power was provided by FAPESP Grants No. 2011/18211-2 and No. 2010/50646-6. The work of VST was supported by FAEPEX/PRP/UNICAMP and FAPESP, SS was supported by Instituto Presbiteriano Mackenzie through Fundo Mackenzie de Pesquisa, and ERA was supported by the Spanish DGI and FEDER funds with Grant No. FIS2011-24149, Junta de Andalucía Grant No. FQM225, and EU Integrated Infrastructure Initiative Hadron Physics Project Contract No. RII3-CT-2004-506078.

## APPENDIX A: WIGNER SYMMETRY FOR $NN$

For completeness we recall here some features of the Wigner SU(4) spin-isospin symmetry. It consists of the following 15 generators:

$$T^a = \frac{1}{2} \sum_A \tau_A^a, \quad (A1)$$

$$S^i = \frac{1}{2} \sum_A \sigma_A^i, \quad (A2)$$

$$G^{ia} = \frac{1}{2} \sum_A \sigma_A^i \tau_A^a, \quad (A3)$$

where  $\tau_A^a$  and  $\sigma_A^i$  are isospin and spin Pauli matrices for nucleon  $A$ , respectively, and  $T^a$  is the total isospin,  $S^i$  the total spin, and  $G^{ia}$  the Gamow-Teller transition operator. The quadratic Casimir operator reads

$$C_{\text{SU}(4)} = T^a T_a + S^i S_i + G^{ia} G_{ia}, \quad (A4)$$

and a complete set of commuting operators can be taken to be  $C_{\text{SU}(4)}$ ,  $T_3$  and  $S_z$ ,  $G_{z3}$ . The fundamental representation has  $C_{\text{SU}(4)} = 4$  and corresponds to a single nucleon state with a quartet of states  $p \uparrow$ ,  $p \downarrow$ ,  $n \uparrow$ ,  $n \downarrow$ , with total spin  $S = 1/2$  and isospin  $T = 1/2$  represented by  $\mathbf{4} = (S, T) = (1/2, 1/2)$ . For two-nucleon states with good spin  $S$  and good isospin  $T$  the Pauli principle requires  $(-)^{S+T+L} = -1$  with  $L$  the angular momentum, and thus

$$C_{\text{SU}(4)}^{\text{ST}} = \frac{1}{2}(\sigma + \tau + \sigma\tau) + \frac{15}{2}, \quad (A5)$$

where  $\tau = \tau_1 \cdot \tau_2 = 2T(T+1) - 3$  and  $\sigma = \sigma_1 \cdot \sigma_2 = 2S(S+1) - 3$ .

One has two SU(4) supermultiplets, whose Casimir values are

$$C_{\text{SU}(4)}^{00} = C_{\text{SU}(4)}^{11} = 9, \quad (\text{A6})$$

$$C_{\text{SU}(4)}^{01} = C_{\text{SU}(4)}^{10} = 5, \quad (\text{A7})$$

corresponding to an antisymmetric sextet  $\mathbf{6}_A = (0, 1) \oplus (1, 0)$  when  $L = \text{even}$  and a symmetric decuplet  $\mathbf{10}_S = (0, 0) \oplus (1, 1)$  when  $L = \text{odd}$ . According to  $LSJ$  quantum numbers we have the following supermultiplets:

$$({}^1S_0, {}^3S_1), ({}^1P_1, {}^3P_{0,1,2}), ({}^1D_2, {}^3D_{1,2,3}) \dots \quad (\text{A8})$$

When applied to the  $NN$  potential, the requirement of Wigner symmetry for *all* states implies

$$V_T = W_T = V_{LS} = W_{LS} = 0, \quad W_S = V_S = W_C, \quad (\text{A9})$$

so that the potential may be written as

$$V = V_C + (2C_{\text{SU}(4)}^{\text{ST}} - 15)W_S. \quad (\text{A10})$$

The particular choice  $W_S = 0$  corresponds to a spin-isospin-independent potential, but in this case no distinction between the  $\mathbf{6}_A$  and  $\mathbf{10}_S$  supermultiplets arises.

## APPENDIX B: THE INFRARED CUTOFF LIMIT OF THE SRG

In this Appendix we show that when the kinetic energy is taken as the generator of the SRG transformations the SRG evolved potential becomes the standard reaction matrix, i.e.,

$$V_s(p, p) \rightarrow R(p, p; p), \quad (\text{B1})$$

when there are no bound states. To avoid unnecessary mathematical complications, we will analyze the problem in a discretized form such as Gauss integration points used in the numerical calculation. The SRG equation in the basis where  $T$  is diagonal becomes

$$\frac{dV_{ik}}{ds} = -(E_i - E_k)^2 V_{ik} + \sum_k (E_i + E_k - 2E_l) V_{il} V_{lk}. \quad (\text{B2})$$

The discrete representation has many advantages. One can see that along evolution in the discrete representation one has an infinite number of constants of motion,  $\frac{d}{ds} \text{Tr}(V_s^n) = 0$ , due to the commutator structure of the SRG equation.<sup>1</sup>

The fixed-point solution implies  $\frac{dV_{ik}}{ds} = 0$ , which requires that  $[[T, V], V] = 0$  so that  $V$  and  $[T, V]$  become diagonal in

<sup>1</sup>Mathematically, such a property is ill defined in the continuum limit since even for  $n = 1$  one has  $\text{Tr}(V_s) = \int_0^\infty p^2 V_s(p, p) = \int_0^\infty r^2 dr V(r, r)$ , which for a local potential  $V(r, r') = V(r)\delta(r - r')$  diverges as the momentum cutoff. Also, the trace of a commutator,  $\text{Tr}[A, B]$ , only vanishes when both  $\text{Tr}(AB)$  and  $\text{Tr}(BA)$  are finite, as the choice  $A = p$  and  $B = x$  clearly illustrates, since  $[p, x] = -i\hbar$  and hence  $\text{Tr}[p, x] = -i\hbar \text{Tr}(\mathbf{1}) = \infty$ .

the same basis, not necessarily the one where  $T$  is diagonal, i.e.,

$$V_{\alpha\beta} = v_\alpha \delta_{\alpha\beta}, \quad (\text{B3})$$

$$0 = \sum_\gamma (T_{\alpha\gamma} V_{\gamma\beta} - V_{\alpha\gamma} T_{\gamma\beta}) = T_{\alpha\beta} (V_\beta - V_\alpha). \quad (\text{B4})$$

The second equation requires that for  $\alpha \neq \beta$  then  $T_{\alpha\beta} = 0$ , which means that  $T$  is diagonal also. Therefore  $V_{ij} = v_i \delta_{ij}$ , i.e.,  $V$  is diagonal in the basis where  $T$  is also diagonal. If we write now the Lippmann-Schwinger (LS) equation for the reaction matrix,

$$R(p', p; k) = V(p', p) + \frac{2}{\pi} \int_0^\infty q^2 dq \frac{V(p', q)R(q, p; k)}{k^2 - q^2}, \quad (\text{B5})$$

with this normalization the phase shift in the one-channel case reads

$$R(p, p; p) = -\frac{\tan \delta(p)}{p}. \quad (\text{B6})$$

Note that the SRG actually implies that the phase shift is constant along the evolution, so that one may take any  $V_s$  in Eq. (B5). The discrete version of this equation for the half off-shell  $R$  matrix,  $R_{ij} = R(p_i, p_j; p_i)$ , reads

$$R_{ij} = V_{ij} + \sum_{k \neq j} \frac{2}{\pi} \Delta q q_k^2 \frac{R_{ik} V_{kl}}{p_i^2 - q_k^2}, \quad (\text{B7})$$

where the principal value corresponds to excluding the point in the sum. Thus, for a diagonal potential we get

$$R_{ij} = V_i \delta_{ij}. \quad (\text{B8})$$

Turning to the phase shift and going to the continuum limit we thus obtain the assertion, so that Eq. (36) is obtained. The proof also holds for the continuum limit, provided a momentum cutoff in the integrals is supplemented.

The infrared solution suggests looking for perturbations around it. Actually, we will see now under what conditions these perturbations are stable. If we write

$$V_{ik}(s) = V_i \delta_{ij} + \Delta V_{ij}, \quad (\text{B9})$$

we get to first order in the perturbation

$$\Delta V'_{ik}(s) = (E_i - E_j)(E_i + V_i - E_j - V_j) \Delta V_{ij}(s), \quad (\text{B10})$$

which yields the solution

$$\Delta V_{ij}(s) = \delta_{ij} \Delta V_{ii}(\infty) + \Delta V_{ij}(\infty) e^{-s(E_i - E_j)(E_i + V_i - E_j - V_j)} \Delta V_{ij}(\infty). \quad (\text{B11})$$

The diagonal part is constant as required by the property  $\text{Tr}V(s) = \text{const}$ . To identify this contribution we use again the LS equation and find that  $\Delta V_{ii} = 0$  and  $\Delta V_{ij}(\infty) = R_{ij}$  for  $i \neq j$ . Thus, we get

$$\Delta V_{ij}(s) = (1 - \delta_{ij}) R_{ij} e^{-s(E_i - E_j)(E_i + V_i - E_j - V_j)}, \quad (\text{B12})$$

which provided  $(E_i - E_j)(E_i + V_i - E_j - V_j) > 0$ . Departures from it measure some off-shellness of the potential.



Going to the continuum limit we get for  $p' \neq p$

$$\Delta V_s(p', p) = R(p', p)e^{-s(E_p - E_{p'})[E_p + R(p, p) - E_{p'} - R(p', p')]}, \quad (\text{B13})$$

where for large  $p$  we obtain  $R(p, p) \rightarrow -\delta(p)/p = V(p, p)$ , which means that at high momentum the kinetic energy dominates and the fixed point is stable. If there are no bound states, we have that  $\delta(p)$  never becomes  $\pi/2$  [since Levinson's theorem states that  $\delta(0) - \delta(\infty) = n_B\pi$ , with  $n_B$  the number

of bound states]. However, for a pole at  $p = p_0$  we get

$$R(p, p) = \frac{1}{p_0(p - p_0)\delta'(p_0)} + \text{reg.}, \quad (\text{B14})$$

where reg. means regular contributions, so that for  $p > p_0 > p'$  and  $\delta'(p_0) > 0$  or  $p' > p_0 > p$  and  $\delta'(p_0) < 0$  the solution becomes stable and unstable otherwise. In the  ${}^3S_1$  channel one has  $\delta'(p_0) < 0$ , which means that the corrections increase dramatically for  $p > p_0 > p'$ .

- 
- [1] S. K. Bogner, T. T. S. Kuo, and A. Schwenk, *Phys. Rep.* **386**, 1 (2003).
- [2] L. Coraggio, A. Covello, A. Gargano, N. Itaco, and T. T. S. Kuo, *Prog. Part. Nucl. Phys.* **62**, 135 (2009).
- [3] S. C. Pieper and R. B. Wiringa, *Annu. Rev. Nucl. Part. Sci.* **51**, 53 (2001).
- [4] K. G. Wilson and J. B. Kogut, *Phys. Rep.* **12**, 75 (1974).
- [5] M. C. Birse, [arXiv:1012.4914](https://arxiv.org/abs/1012.4914).
- [6] S. D. Glazek and K. G. Wilson, *Phys. Rev. D* **48**, 5863 (1993).
- [7] S. D. Glazek and K. G. Wilson, *Phys. Rev. D* **49**, 4214 (1994).
- [8] F. Wegner, *Ann. Physik (Leipzig)* **3**, 77 (1994).
- [9] S. Szpigel and R. J. Perry, [arXiv:nucl-th/9906031](https://arxiv.org/abs/nucl-th/9906031).
- [10] S. Szpigel and R. J. Perry, *Quantum Field Theory, A 20th Century Profile*, edited by A. N. Mitra (Hindustan, New Delhi, 2000).
- [11] S. K. Bogner, R. J. Furnstahl, and R. J. Perry, *Phys. Rev. C* **75**, 061001 (2007).
- [12] S. K. Bogner, R. J. Furnstahl, and A. Schwenk, *Prog. Part. Nucl. Phys.* **65**, 94 (2010).
- [13] S. D. Glazek and R. J. Perry, *Phys. Rev. D* **78**, 045011 (2008).
- [14] K. A. Wendt, R. J. Furnstahl, and R. J. Perry, *Phys. Rev. C* **83**, 034005 (2011).
- [15] P. Navratil, R. Roth, and S. Quaglioni, *Phys. Rev. C* **82**, 034609 (2010).
- [16] E. R. Anderson, S. K. Bogner, R. J. Furnstahl, and R. J. Perry, *Phys. Rev. C* **82**, 054001 (2010).
- [17] R. Roth, T. Neff, and H. Feldmeier, *Prog. Part. Nucl. Phys.* **65**, 50 (2010).
- [18] E. D. Jurgenson, P. Navratil, and R. J. Furnstahl, *Phys. Rev. Lett.* **103**, 082501 (2009).
- [19] E. D. Jurgenson, P. Navratil, and R. J. Furnstahl, *Phys. Rev. C* **83**, 034301 (2011).
- [20] E. D. Jurgenson and R. J. Furnstahl, *Nucl. Phys. A* **818**, 152 (2009).
- [21] H. Hergert and R. Roth, *Phys. Rev. C* **75**, 051001 (2007).
- [22] R. Roth, S. Reinhardt, and H. Hergert, *Phys. Rev. C* **77**, 064003 (2008).
- [23] E. Anderson, S. K. Bogner, R. J. Furnstahl, E. D. Jurgenson, R. J. Perry, and A. Schwenk, *Phys. Rev. C* **77**, 037001 (2008).
- [24] J. D. Holt, T. T. S. Kuo, G. E. Brown, and S. K. Bogner, *Nucl. Phys. A* **733**, 153 (2004).
- [25] A. Calle Cordon and E. Ruiz Arriola, *Phys. Rev. C* **78**, 054002 (2008).
- [26] A. Calle Cordon and E. Ruiz Arriola, *Phys. Rev. C* **80**, 014002 (2009).
- [27] E. Ruiz Arriola and A. Calle Cordon, *PoS EFT09*, 046 (2009).
- [28] E. R. Arriola and A. C. Cordon, *AIP Conf. Proc.* **1322**, 483 (2010).
- [29] D. B. Kaplan and A. V. Manohar, *Phys. Rev. C* **56**, 76 (1997).
- [30] E. R. Arriola, [arXiv:1009.4161](https://arxiv.org/abs/1009.4161).
- [31] T. Mehen, I. W. Stewart, and M. B. Wise, *Phys. Rev. Lett.* **83**, 931 (1999).
- [32] F. J. Wegner, *Phys. Rep.* **348**, 77 (2001).
- [33] R. J. Perry, *Phys. Rep.* **348**, 33 (2001).
- [34] S. Kehrein, *The Flow Equation Approach to Many-Particle Systems* (Springer, New York, 2006).
- [35] V. Bach and J. Bru, *J. Evol. Equations* **10**, 425 (2010).
- [36] S. Szpigel, V. S. Timoteo, and F. d. O. Duraes, *Ann. Phys. (NY)* **326**, 364 (2011).
- [37] S. Okubo and R. Marshak, *Ann. Phys. (NY)* **4**, 166 (1958).
- [38] K. Erkelenz, R. Alzetta, and K. Holinde, *Nucl. Phys. A* **176**, 413 (1971).
- [39] N. Kaiser, R. Brockmann, and W. Weise, *Nucl. Phys. A* **625**, 758 (1997).
- [40] E. Epelbaum, W. Gloeckle, and U.-G. Meissner, *Nucl. Phys. A* **671**, 295 (2000).
- [41] K. Holinde and R. Machleidt, *Nucl. Phys. A* **247**, 495 (1975).
- [42] M. M. Nagels, T. A. Rijken, and J. J. de Swart, *Phys. Rev. D* **17**, 768 (1978).
- [43] R. B. Wiringa, V. G. J. Stoks, and R. Schiavilla, *Phys. Rev. C* **51**, 38 (1995).
- [44] V. G. J. Stoks, R. A. M. Klomp, C. P. F. Terheggen, and J. J. de Swart, *Phys. Rev. C* **49**, 2950 (1994).
- [45] D. R. Entem and R. Machleidt, *Phys. Rev. C* **68**, 041001 (2003).
- [46] V. G. J. Stoks, R. A. M. Komp, M. C. M. Rentmeester, and J. J. de Swart, *Phys. Rev. C* **48**, 792 (1993).
- [47] W. Li, E. R. Anderson, and R. J. Furnstahl, *Phys. Rev. C* **84**, 054002 (2011).
- [48] P. Van Isacker, *Rep. Prog. Phys.* **62**, 1661 (1999).
- [49] S. Baroni, A. O. Macchiavelli, and A. Schwenk, *Phys. Rev. C* **81**, 064308 (2010).